
Hydrogeology of the vicinity of Homestake mine, South Dakota, USA

Larry C. Murdoch · Leonid N. Germanovich ·
Herb Wang · T. C. Onstott · Derek Elsworth ·
Larry Stetler · David Boutt

Abstract The former Homestake mine in South Dakota (USA) cuts fractured metamorphic rock over a region several km² in plan, and plunges to the SE to a depth of 2.4 km. Numerical simulations of the development and

dewatering of the mine workings are based on idealizing the mine-workings system as two overlapping continua, one representing the open drifts and the other representing the host rock with hydrologic properties that vary with effective stress. Equating macroscopic hydrologic properties with characteristics of deformable fractures allows the number of parameters to be reduced, and it provides a physically based justification for changes in properties with depth. The simulations explain important observations, including the co-existence of shallow and deep flow systems, the total dewatering flow rate, the spatial distribution of in-flow, and the magnitude of porosity in the mine workings. The analysis indicates that a deep flow system induced by ~125 years of mining is contained within a surface-truncated ellipsoid roughly 8 km by 4 km in plan view and 5.5 km deep with its long-axis aligned to the strike of the workings. Groundwater flow into the southern side of the workings is characterized by short travel times from the ground surface, whereas flow into the northern side and at depth consists of old water removed from storage.

Received: 2 November 2010 / Accepted: 24 July 2011
Published online: 11 October 2011

© Springer-Verlag 2011

L. C. Murdoch (✉)
Environmental Engineering and Earth Science Department,
Clemson University,
340 Brackett Hall, Clemson, SC 29631, USA
e-mail: lmurdoc@clemson.edu
Tel.: +1-864-6562597

L. N. Germanovich
School of Civil and Environmental Engineering,
Georgia Institute of Technology,
Mason 212 Building, Atlanta, GA 30332, USA
e-mail: leonid@ce.gatech.edu

H. Wang
Department of Geosciences, A254 Weeks Hall,
University of Wisconsin, Madison,
1215 West Dayton Street, Madison, WI 53706-1692, USA
e-mail: wang@geology.wisc.edu

T. C. Onstott
Department of Geosciences,
Princeton University, Guyot Hall, Princeton, NJ 08544, USA
e-mail: tullis@Princeton.EDU

D. Elsworth
Department of Geosciences,
Penn State University,
231 Hosler Building, University Park, PA 16802-5000, USA
e-mail: derek.elsworth@psu.edu

L. Stetler
Geology and Geological Engineering Department,
South Dakota School of Mines,
501 E. St. Joseph St, Rapid City, SD 57701, USA
e-mail: lsetler@taz.sdsmt.edu

D. Boutt
Department of Geosciences,
University of Massachusetts-Amherst,
248 Morrill IV-South, 611 North Pleasant Street, Amherst, MA
01003-929, USA
e-mail: dboutt@geo.umass.edu

Keywords Groundwater flow · Subsidence · Crystalline rocks · Fractured rocks · USA

Introduction

The Homestake mine in South Dakota (USA) was active for 125 years and became one of the deepest and most productive gold mines in North America (Mitchell 2009). The last ore was hauled up the access shafts in 2002 and since then the mine workings have been evaluated as a site for scientific experiments in physics, hydrogeology, microbiology, engineering and other disciplines. The site evaluation was supported by the National Science Foundation as they developed plans for the Deep Underground Science and Engineering Laboratory (DUSEL). Planning of experiments for DUSEL has been on-going by the scientific community for the past decade.

An exploration program associated with mining operations resulted in detailed understanding of the geology, particularly the geologic units containing gold (Caddey et al. 1991). However, compared to aspects of the rock structure, stratigraphy, and petrology, the hydrogeology of

the Homestake mine and encompassing region is relatively poorly known. The lack of hydrogeologic information has hampered the process of planning experiments for DUSEL and was a primary motivation for this investigation. The future of DUSEL is unclear as of this writing, so the site will be referred to in the following pages as the former Homestake mine.

The objective of this paper is to characterize the hydrogeologic parameters in the vicinity of the former Homestake mine by modeling extant data derived from the effects of historical operations at the mine. Furthermore, implications of this model are presented regarding the interactions between the shallow local hydrologic flow systems and the deeper flow systems affected by the mined-out cavities.

Setting

The former Homestake gold mine is near the center of the Lead dome, a structural high roughly 20 km in diameter at the northern end of the Black Hills in western South Dakota. Both the Lead dome and the Black Hills to the south expose Proterozoic metamorphic rocks, which are draped by Paleozoic sediments and cut by Laramide-age igneous intrusions (Dewitt et al. 1986).

Geology

Rocks encompassing and enveloping the former mine are a compositionally diverse package of phyllite and schist that was metamorphosed from greenschist to amphibolite facies and highly deformed during the Proterozoic (Fig. 1; Caddey et al. 1990; 1991). The general structure consists of the Lead anticlinorium and synclinorium, and the Poorman anticlinorium to the west. The longest wavelength of these folds is of the order of kilometers, and their axes plunge 35–50° to the southeast. Rock units within these folds are themselves highly folded at scales ranging from centimeters to 100s of meters. These secondary folds



Fig. 1 Steeply dipping bedding and schistosity in metamorphic rocks near Lead, South Dakota, USA

are so tight that their amplitudes can be many times greater than their wavelengths and their limbs are essentially parallel (Fig. 1). For example, the amplitude of the 15-Ledge fold is more than 1 km, but its wavelength is less than 100 m in the cross-section shown in Caddey et al. (1991, fig. J5).

Regional foliation is roughly parallel to the axial planes of the folds, with a strike approximately N20W and a steep dip to the NE (Rahn and Roggenthen 2002; Fig. 1). Ductile shear zones are also oriented roughly parallel to the regional foliation (Caddey et al. 1991). Despite the complex folds in the vicinity of the Homestake mine, the orientation of the foliation is remarkably uniform across the region.

Gold ore occurred in the hinges of secondary synforms, which plunge ~40° to the SE approximately parallel to the strike of foliation (Caddey et al. 1991). An open pit was dug to recover shallow ores (Fig. 2) and the current town of Lead, SD inhabits its southern side. Miners followed this ore trend to depth, so the underground mine workings

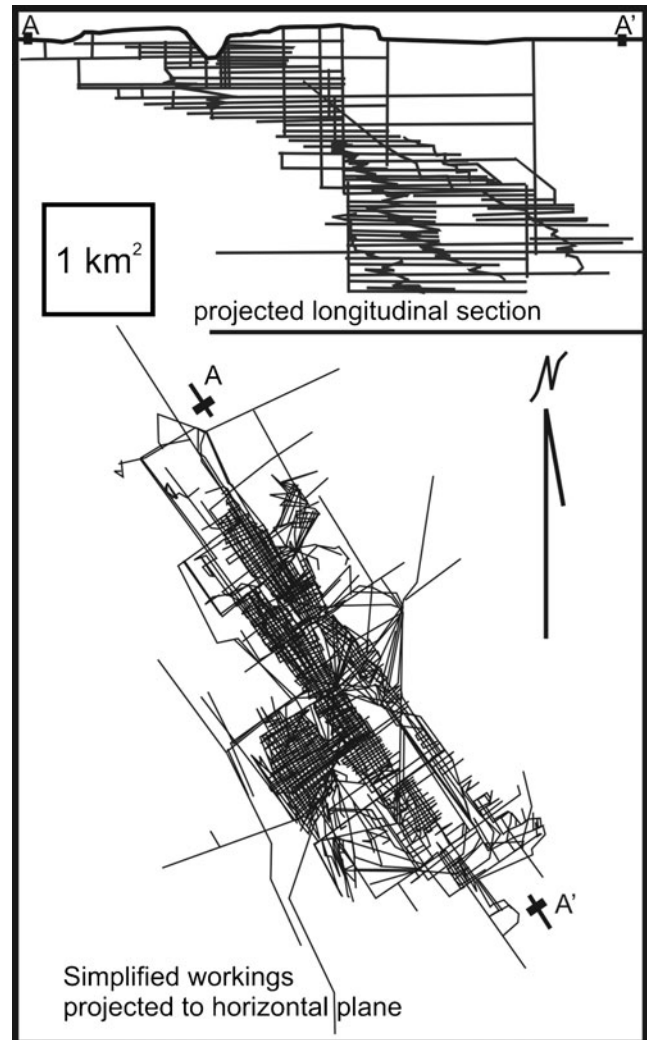


Fig. 2 Cross-section and map of tunnels and shafts comprising the workings at the former Homestake mine. Cross section based on Davis et al. (2009)

at deeper levels are consistently offset to the southeast from the levels above (Fig. 2).

The mine

The mine consists of several hundreds of kilometers of tunnels and stopes contained within a volume of several km³. The plan view area of the workings ranges over several km² at any given level and it extends to a depth of 2.4 km as an irregular, inclined column plunging at ~40° to the SE (Fig. 2). Individual levels of the mine are spaced 30 m apart in the upper levels and 45 m apart below 300 m. The regions between the horizontal workings are cut by myriad boreholes and stopes.

The mine evolved over approximately 125 years (Mitchell 2009; Fielder, 1970), and it is expected that the current hydrologic conditions are a product of that history. Mine workings grew in a complex pattern of advancing depth and lateral spreading as new ore was discovered and removed. Nevertheless, the depth of the mine increased at a remarkably uniform rate of 26 m/yr until maximum depth was reached in 1975 (Fig. 3). Pumps were used to remove the inflowing water, so it follows that the water level in the mine decreased roughly 26 m/yr until 1975 and it was maintained at that level until the dewatering pumps were turned off in 2003. The water level rose quickly over the next 5 years, and it was tracked by monitoring the times when electrical circuits at various levels shorted out. Dewatering was resumed in 2008, and the resulting fall in water level was monitored with a pressure transducer installed at depth (Davis et al. 2009; Zhan and Duex 2010).

Surface hydrologic budget

The vicinity of the former Homestake mine is characterized by an active surface hydrologic system overlying a low permeability formation with slight ambient flow (Driscoll and Carter 2001; Davis et al. 2003; Rahn and Roggenthen 2002). The average annual precipitation is 0.7 m (2.22×10^{-8} m/s), the wettest in the Black Hills

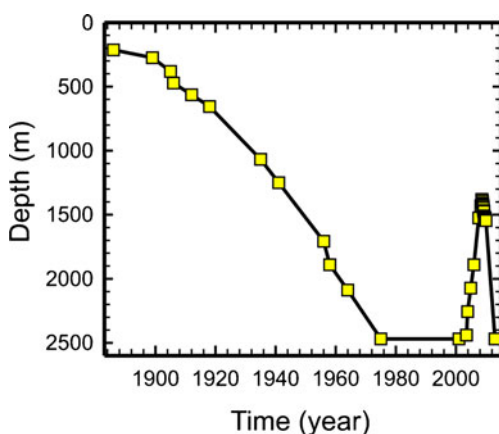


Fig. 3 Depth-to-water in the Homestake mine as a function of time (yellow squares) from Fielder 1970, Zhan 2002 Mitchell 2009. Connecting line segments were used in the analysis

(Driscoll and Carter 2001). Perennial streams are spaced on the order of 1 km (Fig. 4), and are characterized by baseflow ranging from 0.4 to 0.7 of their total flow (Driscoll and Carter 2001).

A hydrologic budget was estimated from a 10-year-long record of stream flow from Whitetail Creek (station 06436156), a 15-km² drainage a few kilometers southwest of Lead, SD. The average total flow (normalized to watershed area) in Whitetail Creek is 8.5×10^{-9} m/s, which is roughly one third (0.37) of the average precipitation, and base flow is 5.2×10^{-9} m/s (Driscoll and Carter 2001). These values were confirmed using a hydrograph separation technique (Gustard et al. 1992; Institute of Hydrology 1980; Rutledge 1998).

The long-term average recharge flux is assumed to be 5.2×10^{-9} m/s (0.16 m/yr), which is equal to the average baseflow. This requires that groundwater does not flow to another watershed. It is possible for recharge to differ from baseflow in areas where the groundwater divide differs from the surface water divide, and this certainly occurs in areas of the Black Hills underlain by karstified limestone (Driscoll and Carter 2001). However, much of the Whitetail Creek watershed is underlain by metamorphic rocks, so the potential confounding effect of karst on the water budget is ignored here.

Hydrogeologic conceptual model

The conceptual hydrogeologic model consists of a dome of low permeability rocks flanked and partly overlain by more permeable rocks (Fig. 5). The surface hydrology consists of perennial streams at kilometer spacing (Carter et al. 2002), so it is assumed that surficial material is more permeable and porous than underlying rocks. The surficial material could be sedimentary rocks overlying the metamorphic basement, but it also could consist of metamorphic rocks that contain fractures with wider apertures or closer spacing than the metamorphic rock at depth. Recharge to the shallow flow system is assumed to be consistent with the baseflow observed in the streams.

The mine is an intricate network of tunnels and borings, and even though the geometry of the network is fairly well known, it is too complex to represent explicitly at the scale of many kilometers. Although extensive, the 500-km of tunnels, mine workings, and back-filled stopes are estimated to occupy less than 1% of the gross volume of the mine workings (Zhan 2002). Therefore, the mine-workings volume is idealized as two overlapping continua, one representing the open drifts and the other representing the country rock left in place. This will enable a simple assumption regarding the water flux from/to the drifts and the country rock (cf. Warren and Root 1963).

Lowering the water level at the mine is expected to have captured groundwater flow in a region that expanded outward to affect the general vicinity of the mine. Continued mining and dewatering would have induced downward flow of water from the shallow flow system toward the mine as well as flow from greater depths where water has been removed from storage (Fig. 5).

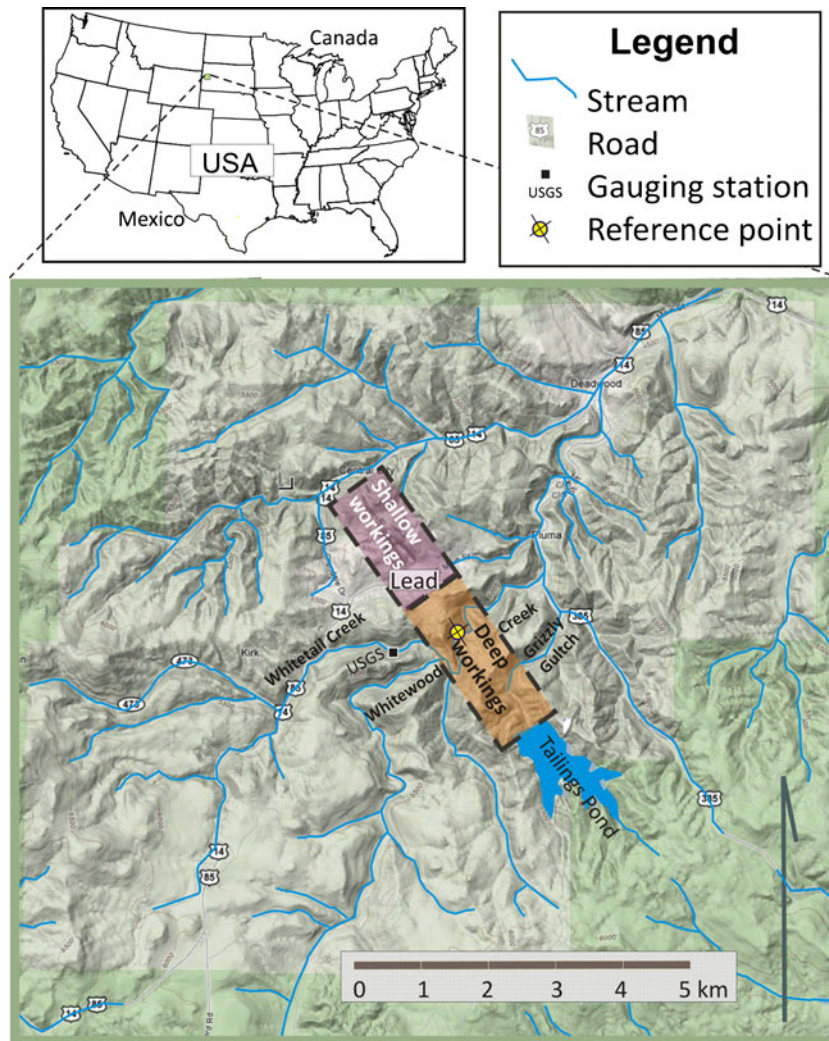


Fig. 4 Mine workings projected onto map of the vicinity of Lead, SD. *Yellow circle with cross* is projection of vertical reference line in the numerical model

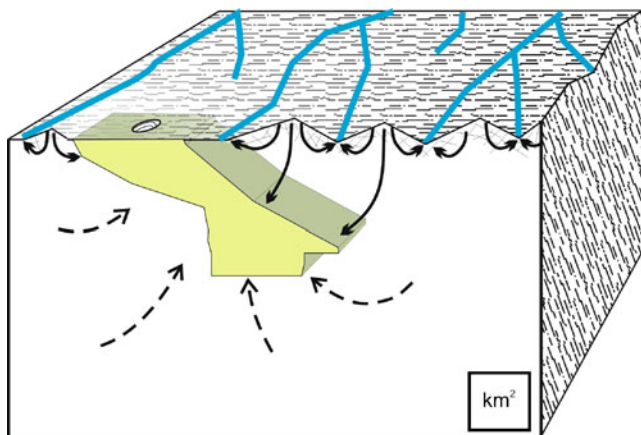


Fig. 5 Hydrogeologic conceptual model of the vicinity of the former Homestake mine (*green*) looking ENE showing the shallow hydrologic system overlying the deep system. *Solid arrows* are flow lines originating as recharge and *dashed lines* are flow released from storage

Numerical modeling

Field data needed to characterize the hydrogeologic conceptual model (Fig. 5) are sparse, so numerical models are developed to provide additional insights. One analysis represents the region as a two-dimensional cross section, whereas the other considers a three-dimensional domain. The general approach will be to represent the mine workings and the rock as two separate, overlapping continua, which occupy the same volume and can exchange water. This allows the problem to be tractable compared to discretizing the tunnels individually.

The two-dimensional (2-D) analysis and most of the three-dimensional (3-D) analyses will be conducted using methods developed to study the pressure and flow of groundwater in aquifers. These will be termed “hydrologic” analyses because they use methods typical of groundwater hydrology. An additional 3-D poroelastic analysis will be conducted to estimate deformations resulting from changes in fluid pressure.

Geometry and mesh

The geometry of the mine is represented as an irregular polygon that encompasses most of the mine workings (Fig. 6). The region representing the workings is a dual-porosity subdomain of crystalline rocks and an excavation network. The whole problem domain extends 20 km across, which is the approximate diameter of the Lead dome (Fig. 6).

The 3-D model is shaped like a half cylinder with the region representing the mine workings at the center. The workings are represented in 3-D by projecting the outline in Fig. 6a as a horizontal prism. The mine workings are assumed to be contained in a region that is symmetric about a vertical plane. Bedding and schistosity create a fabric that is steeply dipping (dips of 60° or greater), and for simplicity, it will be assumed that this fabric is vertical. These assumptions imply that the overall system is symmetric about a vertical plane, so only one half of it is simulated.

An unstructured mesh of approximately 10^4 triangular (2nd order) elements is used for the 2-D hydrologic model and 10^5 tetrahedral elements in the 3-D model. The minimum element span in the region representing the mine is 50 m in the 2-D model and 120 m in the 3-D model. The 2-D model includes small mesh elements near the ground surface to facilitate simulation of the shallow flow system (Fig. 6b). Approximately 10^4 mesh elements were used in the 3-D poroelastic analysis. The extra degrees of freedom in the poroelastic analysis required the use of a mesh that was coarser than the hydrologic analysis.

Governing physics

The mine workings and the fractured rock are assumed to be continuous domains occupying the same volume (Warren and Root 1963). The domain representing the workings advances with time to simulate mining, and water can flow between the domains based on the relative magnitudes of hydraulic head.

Rock domain

In the hydrologic analyses, the rock domain will be simulated combining mass and momentum balances used in groundwater hydrogeology (Bear 1979; Wang and Anderson 1982; Anderson and Woessner 1992):

$$\nabla \cdot (K \nabla h) = S_s \frac{\partial h}{\partial t} - R \quad (1)$$

where $h = P/\gamma + z$ is hydraulic head [basic units: L], K is the hydraulic conductivity tensor [L/T], S_s is the specific storage coefficient [1/L], R is a fluid source term [1/T], P is pore pressure [M/LT²], γ is unit weight of water [M/L²T²], and z is the vertical coordinate [L].

The poroelastic analysis also uses Eq. (1) with modifications to S_s and R , and it is complemented by (Biot 1941; Detournay et al. 1993; Bai and Elsworth 2000; Wang 2000) the coupling relation

$$\frac{E}{2(1+\nu)} \nabla^2 u_i + \frac{E}{2(1+\nu)(1-2\nu)} \frac{\partial \varepsilon}{\partial x_i} = \alpha \gamma \frac{\partial P}{\partial x_i} \quad (2)$$

where u_i is displacement of the solid in the i th direction [L], ε is volumetric strain, E is the drained Young's modulus [M/LT²], α is the Biot-Willis coefficient, and ν is the drained Poisson's ratio. Hereafter, x_i is the spatial coordinates and the 'i' subscript is incremented from 1 through 3 to indicate coordinate directions. The material properties in Eq. (2) consider effects of fractures and matrix lumped together.

Mine workings

The depth of the water in the mine, h_w , can be inferred from historical records (Fig. 3). Hydraulic head in the mine domain, h_m , is determined by assuming the pressure head in air-filled workings is zero (atmospheric), so

$$h_m = z \quad (0 > z > h_w) \quad (3)$$

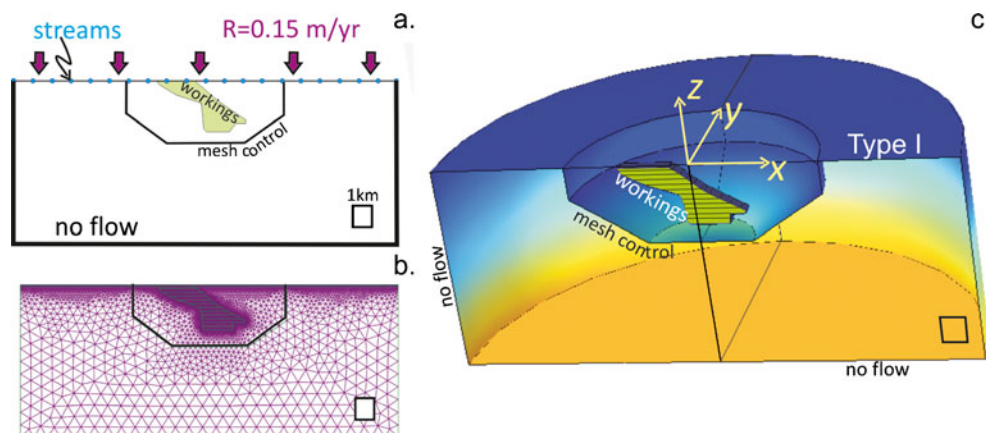


Fig. 6 Configurations of the numerical models. **a** Boundary conditions and geometry of 2-D model. **b** Mesh used in 2-D. **c** Geometry and boundary conditions used in 3-D. Symmetry is assumed, so only half the region is simulated. The coordinates are aligned with the plane of symmetry. The vertical line (z axis) through the workings is used for reference (e.g. Fig. 4). Surface encompassing the workings is used to control the size of the mesh

using coordinates defined in Fig. 6c. This is satisfied if the walls of the workings are covered by a film of water. Drying from the ventilation system would lower the head in the workings, but this is ignored in the current model.

The lower reaches of the mine filled with water after 2003, and it will be assumed that the hydraulic head in the flooded part of the workings is equal to the elevation of the free surface of the water

$$h_m = h_w (h_{wmin} < z \leq h_w, t > 2003) \quad (4)$$

where h_{wmin} is the minimum (deepest) water level (-2,400 m).

The approach outlined above makes use of the high permeability of the mine workings by assuming that the horizontal hydraulic head gradients in the large, karst-like conduits are negligible. As such, the horizontal flow within the mine workings is omitted from this formulation.

Coupling between the domains

Coupling between the rock and the mine domains is accomplished using the source term in Eq. (1) with an approach resembling that used for dual porosity media with two scales of permeability (Barenblatt et al. 1960; Warren and Root 1963; Elsworth and Bai 1992)

$$R = C_g(h_m - h) \frac{\bar{K}}{L^2} \quad (5)$$

where L is a characteristic spacing between tunnels, and C_g is a constant that depends on geometry, \bar{K} is average hydraulic conductivity (scalar). The workings occupy a region of approximately $V_w=5 \text{ km}^3$, and they consist of approximately $L_d=500 \text{ km}$ of tunnels, so the average spacing is assumed to be

$$L \sim \sqrt{V_w/L_d} = 100m \quad (6)$$

The geometric constant, C_g , depends on the shape and spacing of the tunnels. For example, if the tunnels are parallel and evenly spaced, then the characteristic time required for head affected by adjacent tunnels to interact is

$$\tau \approx \frac{S_s L^2}{\bar{K}} \quad (7)$$

Each tunnel behaves like a line sink where the inflow rate is assumed constant for a duration of τ . Integrating the Jacob (1940) log approximation to a transient line source, the space-time average hydraulic head change in the formation at $t=\tau$ is

$$\Delta h \approx \frac{\ln(2.25)}{4\pi} \frac{\Delta Q'}{\bar{K}} \quad (8)$$

where $\Delta Q'$ is the change in flow rate per unit length of the tunnel. Solving Eq. (8) for $\Delta Q'$ and normalizing by the

volume of the formation per unit length of each tunnel, L^2 , gives $C_g=4\pi/\ln(2.25)\approx 15.6$ in Eq. (5).

Coupling between the domains in the poroelastic analysis

The poroelastic analysis includes full coupling between deformation and fluid pressure, which implies that the volumetric strain rate of the solid contributes as an additional fluid source to that given by Eq. (5) for hydrologic analysis. As a result, the poroelastic analysis uses

$$R = C_g(h_m - h) \frac{\bar{K}}{L^2} - \alpha \frac{\partial \varepsilon}{\partial t} \quad (9)$$

as a source term in Eq. (1).

An important consequence of the formulation outlined above is that while water can flow between the rock and mine-workings domains, the analysis does not explicitly consider flow within workings. Rather, the mine-workings are assumed infinitely transmissive and equilibrate immediately to the prescribed head boundary conditions set within the mine. Although this does not allow flow rates to be explicitly evaluated within the mine workings, it is nevertheless a suitable representation of the different response rates of the two media.

Boundary conditions

The boundary conditions in the 2-D problem consist of no-flow conditions along the bottom and sides, and specified flux equal to the recharge rate along the top of the simulated domain (*recharge flux*=0.16 m/yr; Fig. 6a). The hydraulic head is specified and set to 0 at points spaced 1 km apart along the upper boundary to represent streams (Fig. 6a).

Boundary conditions in the 3-D problem consist of a uniform specified-head condition (type I boundary condition) at the ground surface. This is justified because the hydraulic head in the 2-D model varies only by 10s of meters at a depth of 100 m. This variation is small at the scale of the mine, so it seems reasonable to assume the head is uniform as an initial evaluation. The disadvantage of this approach is that the 3-D model ignores details of the shallow flow system, although it allows the exchange of water between the shallow and deep flow systems to be estimated. The advantage is that it reduces the execution time by reducing the size of the mesh, and this was done to facilitate solution of the problem. Boundary conditions along the sides and bottom of the 3-D model are zero flux.

Fluid boundary conditions in the poroelastic analysis are the same as in the hydrologic analysis. The mechanical boundary conditions assume fixed displacement along the base, and roller boundary conditions along the vertical sides of the 3-D region (Fig. 6). The total stress is zero at the upper surface.

Rock properties

Rock properties are estimated from studies within the mine, from regional evaluations, and from studies of similar rocks elsewhere (Table 1). Rock properties vary within the vicinity of Homestake, but it is assumed that at the scale of the model, the hydrologic and mechanical properties of the rock are dominantly controlled by rock layering and stress. The orientation of the schistosity and layering appears to be fairly consistent across the region and some faults and fractures also follow this trend (Rahn and Roggenthen 2002); therefore, it is assumed that properties at a given depth are uniform, but vary with depth as a result of changes in effective stress.

The hydrologic analysis requires knowledge of the hydraulic conductivity, K , specific storage coefficient, S_s , and effective porosity, n_e . It is assumed that these properties are dominated by the effects of fractures. This allows macroscopic parameters to be estimated using basic characteristics of the fracture network defined by a fracture density ψ (fracture area/volume of enveloping rock), and an average hydraulic aperture δ . The reciprocal of ψ is the average fracture spacing. The average hydraulic conductivity is (e.g., Bear 1979)

$$K = \frac{\psi \delta^3 \gamma}{12\mu} \quad (10)$$

assuming the fractures are parallel.

Bedding and schistosity of rocks at Homestake create a fabric that likely causes the hydraulic conductivity to be anisotropic. The strike of the rock fabric is approximately aligned with the N20W axis of the mine. The dip is steep (60° or greater) to the NE, so to simplify the analysis, the authors assume layering defining the fabric is vertical. This allows the principal axes of the anisotropy to be aligned with the coordinate axes. Rahn and Johnson 2002 concluded that $K_{\max}/K_{\min} \approx 5$ at a nearby site underlain by foliated metamorphic rocks that are similar to the rocks in the vicinity of Homestake. There is no information about the anisotropy in the vicinity of Homestake, so the

authors follow Rahn and Johnson 2002 and assume $K_{\max}/K_{\min} \approx 5$. This was accomplished by calculating $K_x = K_z = K$ using Eq. (10) and setting $K_y = K/5$, where the x-direction is along strike N20W (Fig. 6).

Effective porosity is assumed to be

$$n_e = \psi \delta \quad (11)$$

The storage coefficient for the hydrologic analysis is the unconstrained specific storage, S_σ , which is given by,

$$S = S_\sigma = \gamma(1/K_b + \psi \delta \beta) \quad (12)$$

where β is the compressibility of water, K_b is the bulk modulus of the fractured rock, and it is implied that changes in the principal stresses due to changes in fluid pressure are independent of direction ($d\sigma_{xx} \approx d\sigma_{yy} \approx d\sigma_{zz}$) (Doe et al. 1982; Rutqvist 1995; Rutqvist et al. 1997; Svenson and Schweisinger 2007). The bulk modulus in Eq. (12) is assumed to have components from deformable fractures and solid rock

$$\frac{1}{K_b} = \frac{1}{K_s} + C_n \psi = \frac{3(1-2\nu)}{E_s} + C_n \psi \quad (13)$$

where K_s and E_s are the bulk modulus and Young's modulus of the solid, respectively. C_n is the fracture normal compliance,

$$C_n = \frac{\partial \delta}{\partial \sigma_e} \quad (14)$$

where σ_e is effective stress. The approach in Eq. (13) uses the simplifying assumption that the fractures are randomly oriented and interaction between fractures is ignored (e.g., Germanovich and Dyskin 1994).

Changes in properties with depth

Hydrogeologic properties of fractured rock are expected to change with depth because the increase in effective stress

Table 1 Available estimates of hydrogeologic properties in the vicinity of the former Homestake mine

Property	Value	Method	Source
Hydraulic conductivity	10^{-9} m/s 10^{-8} to 10^{-9} m/s	Pumping test in mine Estimate	Zhan (2002) Davis et al. (2009)
Porosity	0.01	Estimate	Zhan and Duex (2010); Rahn and Roggenthen (2002); Driscoll and Carter 2001; Rahn (1985)
Specific storage	10^{-7} m ⁻¹	General value for fractured crystalline rock	Wang (2000); Domenico and Mifflin (1965)
Young's modulus	90 ^a , 58 ^b , 77 ^c GPa	Average values from laboratory tests	Pariseau (1985, table 21)
Shear modulus	~30 GPa	Average values from laboratory tests	Pariseau (1985)
Poisson's ratio	0.19 ^a , 0.17 ^b , 0.10 ^c	Laboratory studies on core from mine	Pariseau (1985, table 21)

^a Parallel to dip direction

^b Normal to schistosity

^c Parallel to strike

closes the fractures and makes them stiffer. One approach to predicting this effect is to assume a relationship between aperture and effective stress acting on the fractures. Several such relationships have been described (Jaeger et al. 2007; Bai and Elsworth 2000; Ruqvist and Stephansson 2003), and according to Ruqvist and Stephansson 2003, the most common one is

$$\delta = \delta_o + \frac{(\delta_o - \delta_{\min})C_{ni}\sigma_e}{\delta_o - \delta_{\min} - C_{ni}\sigma_e} \quad (15)$$

where δ_o is the contact aperture, δ_{\min} is the minimum aperture under infinite stress, and C_{ni} is the initial normal compliance (i.e. the normal compliance at zero effective stress) (Bandis and Barton 1983).

The compliance of the fracture can be obtained by substituting Eq. (15) into Eq. (14) as

$$C_n = \frac{C_{ni}(\delta_o - \delta_{\min})^2}{(\delta_o - \delta_{\min} - C_{ni}\sigma_e)^2} \quad (16)$$

Effective stress is defined by

$$\sigma_e = \sigma_T + \alpha_f P \quad (17)$$

where σ_T is the total stress (tensile stresses are positive), P is pore pressure, and α_f for a single fracture is the ratio of open area to the total area of the fracture surface (Murdoch and Germanovich 2006). In general, α_f of a fractured medium will depend on the characteristics of individual fractures, as well as the fracture density and geometry of the fracture network. For simplicity and to reduce the number of parameters, it is assumed that $\alpha_f = \alpha$.

The initial vertical effective stress prior to mining is estimated as

$$\sigma_{ei} = -(\gamma_r - \gamma_w)d \quad (18)$$

where γ_r and γ_w are the unit weights of rock and water, respectively, d is depth, and the vertical and horizontal stresses are assumed equal and as such lack a tectonic component or horizontal displacement restraint. Substituting Eq. (18) into Eqs. (10)–(16) gives the initial distribution of macroscopic hydrologic properties with depth. Changes in effective stress are determined in the hydrologic analysis by assuming no change in total stress (σ_T) in Eq. (17), so only changes in pore fluid pressure (P) affect effective stress.

Poroelastic properties

The poroelastic analysis is conducted using the parameters: drained bulk Young's modulus E_b ; drained Poisson's ratio, ν ; hydraulic conductivity, K ; Biot-Willis coefficient, α ; and the Biot modulus, M . The drained bulk Young's modulus is determined as

$$E_b = E_s \frac{1}{1 + \theta} \quad (19)$$

with

$$\theta = \frac{E_s C_n \psi}{3(1 - 2\nu)} \quad (20)$$

which follows from Eq. (13). Neglecting the effects of the difference between Poisson's ratios of the fractured rock and the solid rock gives

$$\alpha = 1 - \frac{K_b}{K_s} \approx 1 - \frac{E_b}{E_s} = \frac{\theta}{1 + \theta} \quad (21)$$

The storage coefficient in Eq. (1) for the poroelastic analysis is (Wang 2000, equation 3.38)

$$S_\varepsilon = \frac{1}{M} = S_\sigma - \frac{3\alpha^2(1 - 2\nu)}{E_b} \quad (22)$$

where S_σ is given by Eqs. (12), (13) and (16), (17) with $\alpha_f = \alpha$.

The effective stress, σ_e , in the poroelastic analysis is determined using Eq. (2) and elastic constitutive relations (e.g. Bai and Elsworth 2000; equation 2.6). The mean principal stress is added to the stress σ_{ei} in Eqs. (15) and (16) in the poroelastic analysis.

The advantage of taking the approach outlined above is that it allows the eight macroscopic properties used in the hydrologic analysis (K , S_s , n_c) and the poroelastic analysis (K_b , M , E_b , ν , α) to be defined by six parameters describing the fracture system (δ_o , δ_{\min} , C_{ni} , ψ) and rock matrix (ν , E_s) (Rutqvist 1995; Ruqvist and Stephansson 2003; Baghbanan and Jing 2008). Five of these parameters (ν , E_s , δ_o , δ_{\min} , C_{ni}) are fairly well constrained or calibrated (see below). This is similar to the concept of effective properties of heterogeneous (fractured) materials (Germanovich and Dyskin 1994) and provides a consistent basis for defining macroscopic properties that reduces the degrees of freedom in the simulations. The aforementioned mathematical problem was solved using the Galerkin finite element method implemented in Comsol Multiphysics software.

Results

The analysis was conducted by running the 2-D and 3-D simulations in several steps. Initial results were obtained using the 2-D analyses (Fig. 7) with preliminary values of parameters based on Table 1. These results showed that the variation in hydraulic head at shallow depths was small at the scale of the model (slopes less than 0.05), and this finding justified the use of constant head conditions on the upper boundary of the 3-D model. The initial set of parameters was then revised manually so the 3-D model best matched the available data. The new parameters were used in the 2-D model to calculate the results shown in the following. The parameters obtained by calibration were remarkably similar to the original estimates, so the original findings from the 2-D model were unaffected.

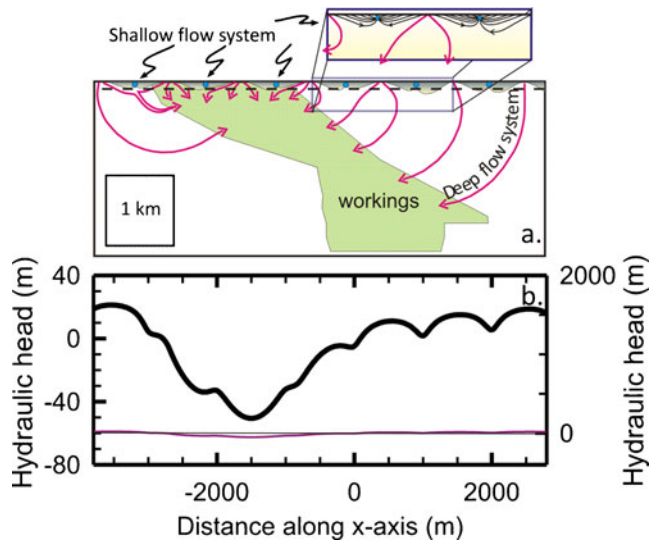


Fig. 7 a Shallow and deep flow systems predicted using the 2-D model. Shallow flow systems are shaded in the cross-section with pathlines shown in the inset. Dashed line is at a depth of 100 m. Blue dots are streams. Flow paths to the deep flow system are in red. b Hydraulic head profile along dashed line in part a. Thick black line plotted with scale on the left, thin purple line plotted with 1:1 scale on the right. Thin black line is a horizontal reference

Parameters obtained by calibrating the hydrologic model were used in the poroelastic model.

Calibration of 3-D model

Values of $\nu=0.2$ and $E_s=75$ GPa were assumed based on values in Table 1 and a value of $\psi=28$ m⁻¹ (fracture spacing ≈ 3.5 cm) was also assumed. The 3-D hydrologic model (Fig. 6c) was then calibrated by adjusting δ_o , δ_{min} , and C_{ni} manually. The flow rate into the mine was estimated as a function of depth in increments of 200 m from the source term R in Eq. (1). Integrating R over volume provided the total flow rate.

The calibration exercise yielded estimates of $\delta_o=30$ μ m, $\delta_{min}=3.8$ μ m, and $C_{ni}=10^{-10}$ m/Pa. These values give a total flow rate into the mine workings of 0.046 m³/s in the early 1990s. For comparison, the range of water flowing naturally into the mine given by Zhan 2002 and Zhan and Dux 2010 for the same time period was 0.042–0.048 m³/s (Fig. 8). Water was also pumped into the mine, but this flow was identified by Zhan 2002 and omitted from the values given in the previous sentence.

The flow into the mine increases with depth according to both the model results and field measurements given by Zhan 2002. The modeled results overlap the observed inflow rates, except at shallow depths (less than 1 km), where the observed cumulative inflow is less than that predicted by the model (Fig. 9). The poroelastic analysis gives flows that are similar to those of the hydrologic analysis (Fig. 9).

The analysis of the inflow during flooding can be used to provide an estimate of the void volume created by the mining operation. During the 5 years when the water level was rising (2003–2008), the calculated (modeled) total

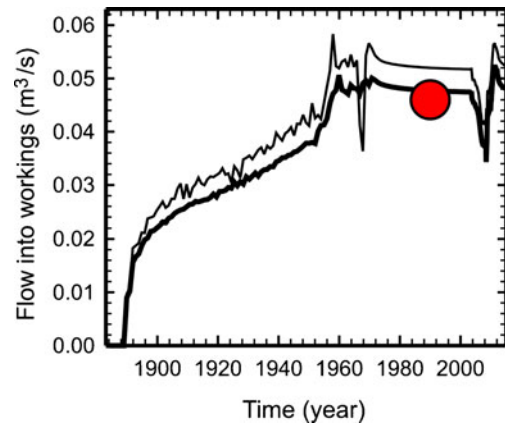


Fig. 8 Total simulated flowrate into mine workings using hydrologic analysis (thick line) and poroelastic analysis (thin line) and the total flow during dewatering according to Zhan 2002 (red circle)

volume of water that flowed into the mine is 6.5×10^6 m³. This volume of water fills the voids created by mining operations. The total volume of the region representing the lowest 1 km of the mine in the model is 1.78×10^9 m³. In the absence of dewatering, this indicates that the normalized void volume (volume of voids created by mining/total volume of enveloping rock) of the lowest 1 km of the mine is 0.0036.

For comparison, Zhan (2002; figure 3.4) gives an estimate of the void volume remaining at the end of mining to be 5×10^6 m³ (4,000 acre ft) between 1,400 and 2,400 m. This corresponds to a normalized void volume of 0.0028. Rahn and Roggenthen (2002) estimated the total volume of voids created by overall mining operations to be 2.1×10^7 m³, and the total volume of the mine in the model is 3.92×10^9 m³, which gives a normalized void volume of 0.0053. Again, these magnitudes are reasonably similar.

The present simulations indicate a normalized void volume created by mining that is between values given by Zhan (2002) and Rahn and Roggenthen (2002). Given the uncertainty in the estimates of the normalized volume, it is

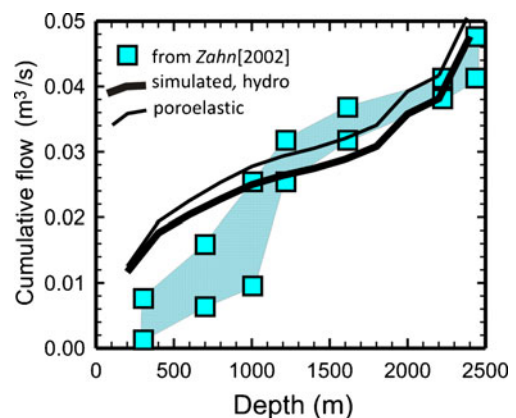


Fig. 9 Cumulative flow into the mine as a function of depth, from hydrologic and poroelastic simulations (lines) and observations by Zhan 2002 (blue squares and shaded band)

concluded that the value determined from the simulations is consistent with the available data.

Distribution of properties

The macroscopic properties can be calculated from parameters obtained through calibration, according to Eqs. (16), (19) and (20). The analysis shows that because the properties are stress-dependent, they change by several orders of magnitude in the upper few hundred meters. The properties are nearly uniform at depths below 1,000 m (Fig. 10) because the effective stress is high and the fracture apertures approach the minimum aperture, δ_{\min} . Values of properties below 1,000 m are similar to values expected from observations at the Homestake site or in the vicinity (Table 1).

The depth dependence of the hydraulic properties before and at the end of mining is also shown in Fig. 10a. The effect of significant changes (~ 10 MPa) in effective stress on hydraulic parameters is remarkably modest because according to Eq. (15) the stiffness of the fractures below a few hundred meters is such that their aperture changes only slightly in response to changes in stress.

Although the field data are sparse, K in Fig. 10 is within an order of magnitude of available estimates (Table 1). The marked increase in hydraulic conductivity with decreasing depth is consistent with the development of a shallow hydraulic system where flow is significantly more rapid than in the deeper system.

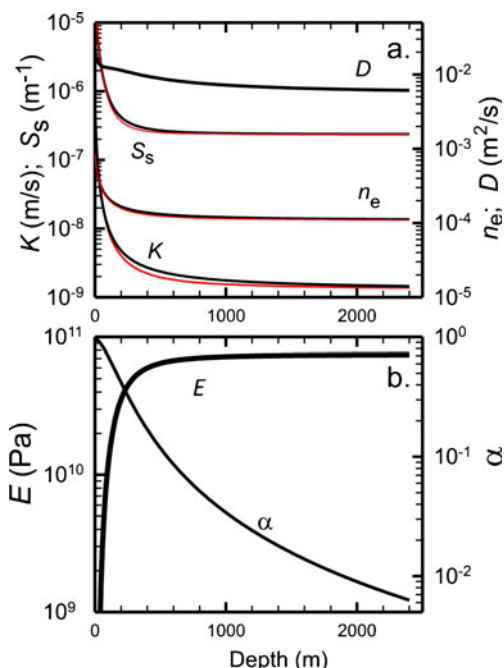


Fig. 10 a Hydraulic conductivity (K), specific storage (S_s), hydraulic diffusivity (D), and effective porosity (n_e) as functions of depth along z axis, according to results of calibration. *Black lines* are initial values, *red lines* are values at the end of mining showing effect of dewatering. b Young's modulus (E) and Biot-Willis coefficient (α) as functions of depth

Shallow flow system

The 2-D model shows the development of both shallow and deep flow systems (Fig. 7a). The shallow flow system consists of recharge that flows laterally to nearby streams. Flow paths are limited to approximately the upper 100 m where K is several orders of magnitude larger than at greater depths (Fig. 7a, inset). Shallow flow systems are present across the entire model, including the area overlying the shallow mine workings.

Flow pathlines in the shallow flow system in the 2-D model extend to depths of 100–140 m, which is consistent with the regional estimate of 150 m for the depth of the shallow aquifer given by Rahn (1985). The maximum hydraulic head between streams is approximately 20 m in the simulations. The topographic relief in the field area is 100–150 m, which bounds the upper limit for the maximum hydraulic head between the streams. The simulations give maximum horizontal head gradients of 0.04–0.05 (Fig. 7b). The hydraulic head drops by about 70 m in the region overlying the shallow workings ($0 < x < 3,000$ m). This gives a horizontal hydraulic gradient of approximately 0.046.

The mine clearly has an effect on the elevation of the hydraulic head in the model, but it is remarkably small compared to the size of the mine. For comparison, Rahn and Johnson (2002) studied the groundwater near Nemo, SD, a town 30 km SE (along strike) of Homestake. The rocks beneath Nemo resemble those at Homestake, but the relief is more subdued, roughly 20 m. Rahn and Johnson (2002, figure 3) show horizontal hydraulic head gradients of 0.01–0.03 in their primary map area, and they infer a head distribution with gradients of 0.06–0.08 in areas of greater relief on the periphery of their study area.

Pathlines roughly midway between the streams extend into the deep subsurface where they curve towards and ultimately discharge into the mine workings. These pathlines represent the interaction between the shallow and deep flow systems. Water that flows from the ground surface to the mine originates as recharge in the uplands between streams. The number of pathlines entering the deep system increases from the edge of the model to the region overlying the shallow workings, indicating an increase in flux to the deep system. However, the flux to the deep system does not capture all of the recharge even directly over the shallow mine workings (Fig. 7a).

Deep flow system

The deep flow system is the region where flow has been affected by operation of the mine. This region evolved as the change in hydraulic head moved downward and the flow system responded to dewatering throughout the operation of the mine (Fig. 11). The deep flow system includes a recharge capture zone where water originating as recharge has flowed along a relatively short and generally downward path into the mine. Underlying this is a storage capture zone where water has traveled along a much longer path and is directed generally upward when captured by the deeper levels of the mine.

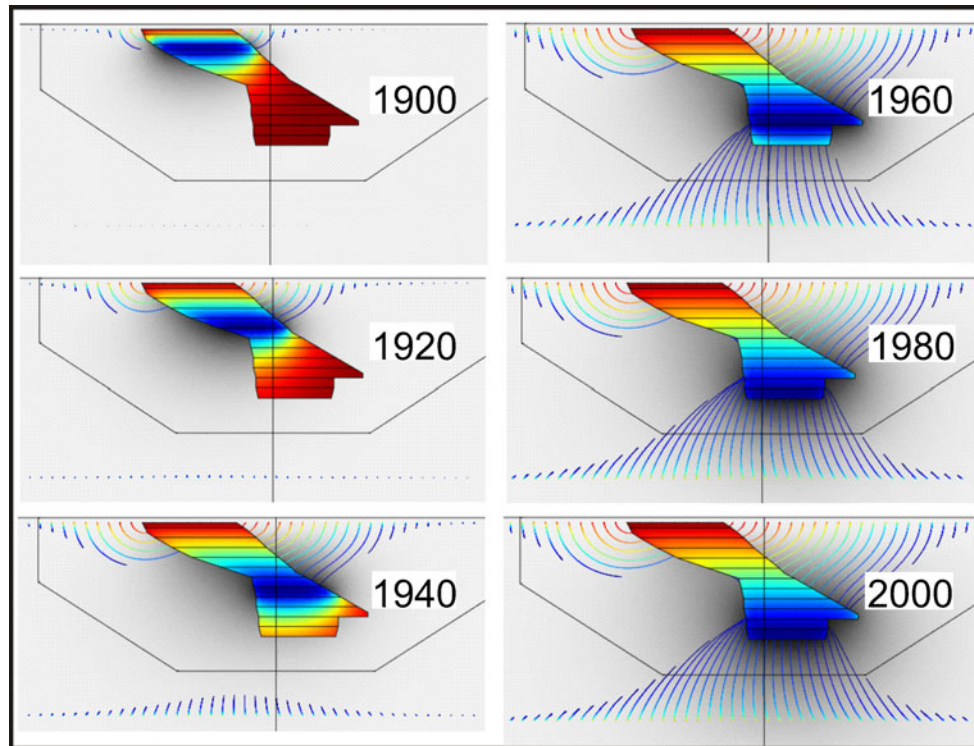


Fig. 11 Hydraulic head (*color flood and grey tone*) and particle paths (*lines*) as function of time (year indicated in each panel). The *colors indicating hydraulic head* are scaled to the maximum change in each panel. *Colors along pathlines* indicate travel time, which is scaled to the time since mining started. *Grey fill* is hydraulic head outside of the mine. The *grey scale* for hydraulic head was used instead of the color flood to highlight pathlines outside the workings

Recharge capture zone

Flow pathways from the ground surface to the mine and travel times along these pathways were calculated using values of n_e determined from Eq. (11) and shown in Fig. 10. The results show that pumping has captured water originating as recharge from distances as far away as several kilometers from the surface expression of the mine. The flow paths are downward and curve toward the mine where they are ultimately captured by the workings at depths of several hundred meters (Fig. 13). The capture zone at the ground surface is roughly elliptical with a major axis of 8,000 m and a minor axis of 4,000 m. Flow paths beyond these distances have been affected by the mine, but the travel time to the mine in this external region is longer than 125 years, so those paths are outside of the recharge capture zone.

The vertical advective flow velocity estimated from Darcy's Law is

$$v_z = \frac{q_z}{n_e} = -\delta^2 \frac{\gamma}{12\mu} \frac{\partial h}{\partial z} \quad (23)$$

The vertical hydraulic head gradient, $\partial h/\partial z$, overlying the mine workings is approximately unity (Fig. 12a). This is a consequence of the pressure head being equal to atmospheric pressure at the top and bottom of this zone. Using Eq. (23) with a fracture aperture $\delta=4 \mu\text{m}$ near δ_{\min} gives a velocity of roughly 1 m/day. Using a fracture aperture $\delta=20 \mu\text{m}$, which is roughly a median

between δ_{\min} and δ_o , gives $v=25$ m/day. The mine workings are 1,600–2,000 m deep along the south side and it appears that the average travel time in this region is one to several years, but it could be on the order of a month or less through localized fractures with apertures of 10s of microns.

A zone of particularly fast travel from the surface to the mine workings occurs in the vicinity of the shallow workings. This zone extends to roughly 0.5 km southeast of the shallow workings with its southeastern edge in the vicinity of Whitewood Creek. The long axis of the 1-year-travel-time zone is 2,600 m and it trends N20W. A larger zone where travel times are less than 10 years has a long axis of 6,000 m, and the 100-yr capture zone spans more than 8,000 m (Fig 13b).

Storage capture zone

The storage capture zone supplies the flow into the lower mine workings. Water is released from storage due to the large decrease in pressure caused by dewatering the mine. The boundary of the storage capture zone is taken as the outer edge of the region from which water has been released from storage and reached the mine. This zone was delineated by tracing many particles paths and identifying the most distant starting positions of paths that reached the mine. This zone is roughly elliptical in shape, with a major horizontal axis of 8,500 m and a minor axis of 4,000 m. The storage capture zone extends

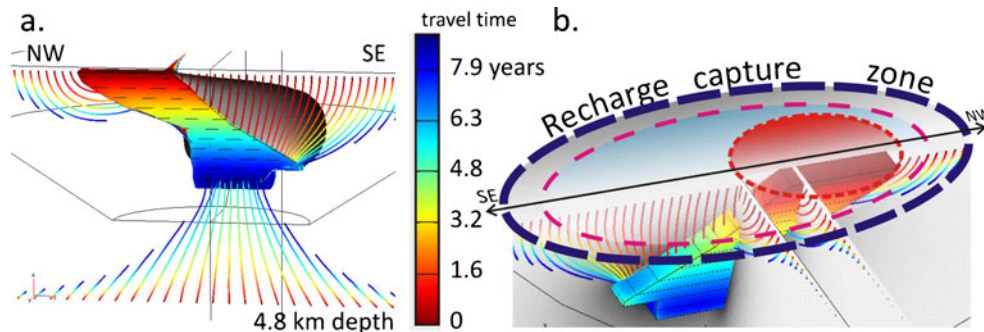


Fig. 12 a Hydraulic head and travel times in 2003. Hydraulic head in the region of the mine workings (colors) scaled to a maximum head change of 2,400 m. Travel time along particle paths indicated by colors and given by scale. Grey tone shading is the region where vertical hydraulic gradient is between 0.5 and 2. b Perspective of mine workings and particle paths with the zones of surface capture. Travel times from the ground surface to the mine range from less than 1 year (in region defined by orange dashed line), 10 years (within pink dashed line) and 120 years (within the purplish-blue dashed line)

to approximately 5,500 m depth, according to the analysis (Fig. 13).

Flow velocity increases as the mine is approached. The workings are tightly enveloped by the 2 m/day isosurface of flow velocity (Fig 13). The velocity isosurface of 0.1 m/day is remarkably close to the current boundary of the storage capture zone. As a result, 0.1 to 2 m/day appear to be the general range of flow velocities in the storage capture zone.

Interaction between the shallow and deep hydrologic systems

Water flows from the shallow to deep systems. The pre-mining flow system has pathlines of a topographically driven system, originally calculated by Toth (1963). In one of Toth's examples, the depth of the basin is 300 m, the stream spacing is 1,600 m, and the amplitude of the maximum head between streams is 70 m. These param-

eters are within a factor of two to three to those in the Black Hills.

The magnitude of the flux from shallow to deep is of interest because it shows the impact that the deep system has on the shallow one. The vertical flux in the 3-D model was calculated at a depth of 300 m and this was scaled to the magnitude of recharge obtained from the hydrologic water budget. The upper boundary condition in the 3-D model assumes constant head, so the magnitude of the vertical flux becomes whatever value is required to meet the conditions imposed by the underlying mine workings.

The vertical flux in the analysis is less than the recharge at a depth of 300 m, with the maximum ratio of the fluxes approximately 0.8. The maximum flux occurs where the workings are shallowest. This result indicates that some recharge flux is available to discharge to streams, even in the vicinity of the shallow workings.

Whitewood Creek crosses over the workings in a region where the maximum flux ratio is approximately 0.6. The implication is that the rate at which Whitewood Creek gains by groundwater discharge is diminished over the workings, but the effect of the mine is insufficient for the stream to lose water. This should be interpreted to mean that loss of water from Whitewood Creek to the mine is unnecessary to explain the available data, but the resolution of the simulation is insufficient to rule out this as a possibility.

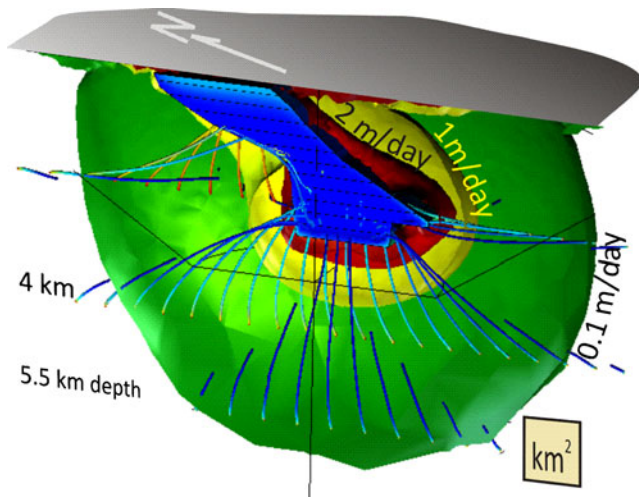


Fig. 13 Perspective of isosurfaces of groundwater flow velocity in 1993 and particle paths since the start of mining (colored lines). The lowest line of pathlines starts at a depth of 5.5 km. Colors on pathlines are scaled to travel time, where blue lines represent the longest time. The isosurface of 0.1 m/day is the approximate envelope of the region over which the mine has captured water from storage during its lifetime. The former mine workings is shown as a blue area. The grey area refers to the ground surface

Deformation

Deformation resulting from pumping was evaluated using the poroelastic analysis outlined in section on numerical modeling and the parameter distributions in Fig. 10. Results show that the magnitude of deformation is particularly sensitive to the magnitude of pressure change and properties, E and α . Dewatering throughout the history of mining results in subsidence over a region roughly the size of the recharge capture zone (Fig. 14), with a maximum displacement of 5 cm at the southern end of the shallow workings ($x=-1,000$ m). The rise in water level from years 2003–2008 causes doming that peaked in 2010 with a maximum amplitude of about 0.2 cm. The maximum

displacement caused by the rise in water level occurs at $x=2,000$ m overlying the deepest part of the mine. The maximum tilt magnitude along the N20W profile in 2010 is approximately $0.4 \mu\text{rad}$.

Discussion

The simulations confirm the general expectations of the conceptual model (Fig. 5) and suggest additional details that improve the resolution of the hydrogeology. It appears that in the vicinity of the former mine workings, four major zones are distinguished by the source and the fate of the water flowing through them. These include the: (1) shallow flow system; (2) recharge capture zone; (3) storage capture zone; and (4) former mine workings (Fig. 15).

The shallow flow system is recharged by infiltration and discharges to local streams and controls active hydrologic processes in the region. By being a hydraulic sink, the mine has significantly affected the deep flow system. Two capture zones—one zone where water is derived from recharge and another where it is removed from storage—have been identified within the region influenced by dewatering. The recharge capture zone is characterized by relatively short flow paths from the shallow flow system into the mine. The maximum vertical flux supplied to the recharge capture zone is 0.8 of the ambient recharge. This implies that water in the shallow

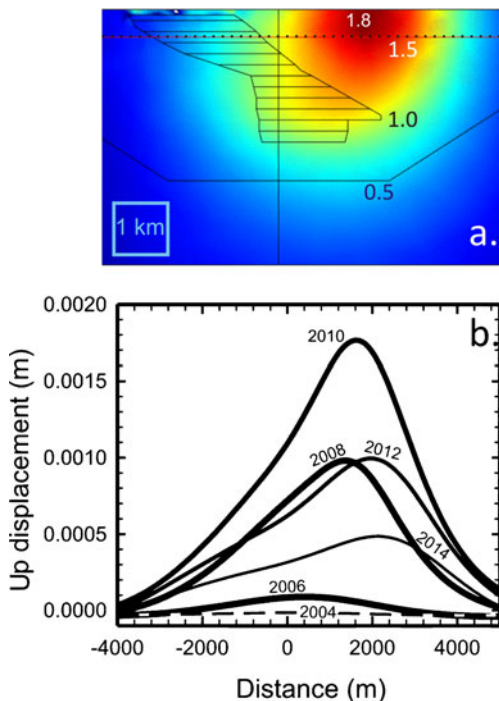


Fig. 14 a Upward displacement from 2003 to 2010 along a cross-section through the N20W axis of the mine workings. Numbers are displacement in m. b Displacement profiles at a depth of 500 m (dotted line in part a.) as a function of time (by year) caused by flooding and dewatering using hydraulic heads in Fig. 3

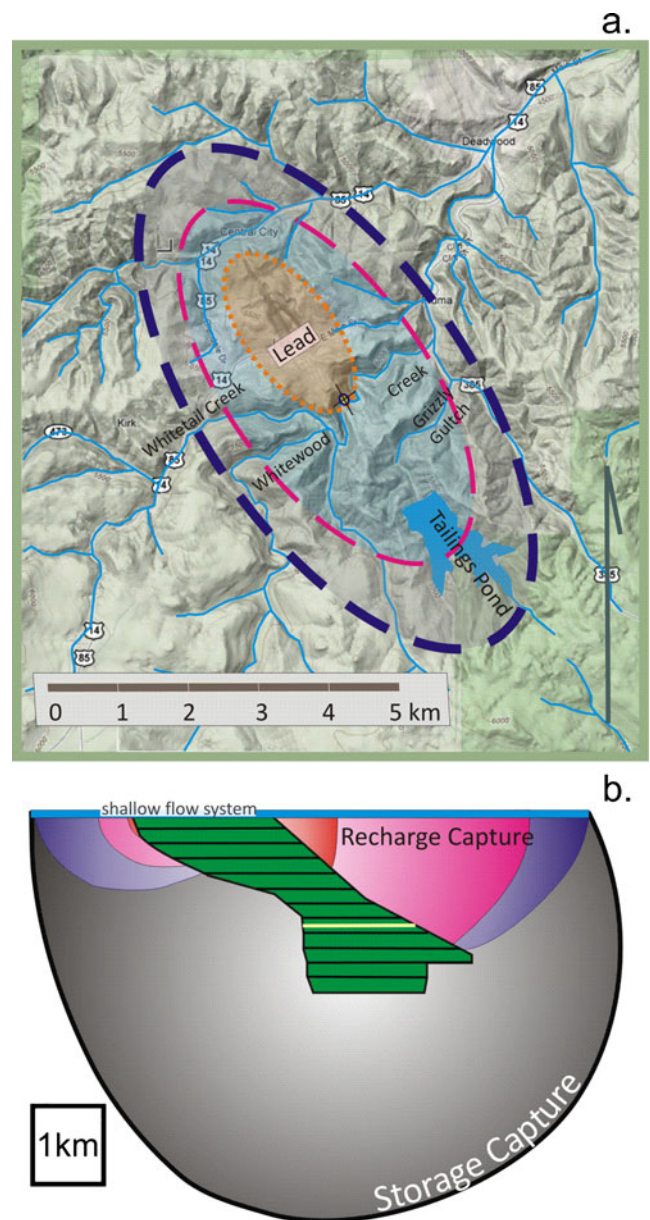


Fig. 15 Hydrogeologic zones in the vicinity of the former Homestake mine in a map and b section views. Mine workings with levels separated by 200 m for scale (green). Yellow line in the mine workings marks 1,500 m depth. Recharge capture zone where travel times are less than 1 yr is approximately within the orange dashed line, 10-yr travel time is within the pink dashed line and 120-yr travel time is within the purplish-blue dashed line. Grey shaded region is where water has been removed from storage. The shallow flow system extends to depths of 100 m (blue)

flow system is diminished, but not depleted by dewatering at the mine (Fig. 7). The recharge capture zone extends to depths of approximately 1,800 m on the southeast side and 800 m on the northwest side of the workings (Fig. 15). Water recovered from below those depths is derived from storage and is characterized by upward flow of older water. The deep flow system receives a fraction of the ambient recharge to the shallow system.

The extent of the recharge capture zone on the surface is roughly elliptical with axes of $8 \text{ km} \times 4 \text{ km}$. Average

travel times are less than 10 years over an inscribed elliptical region roughly $6 \text{ km} \times 3 \text{ km}$ with a zone of fast paths where travel times are less than a year further inscribed within this and roughly $2.5 \text{ km} \times 1.5 \text{ km}$ (Fig. 15). Mine inflow from water released from storage appears to have occurred over a region roughly $8 \text{ km} \times 4 \text{ km}$ that extends to a depth of 5.5 km. The flow of water beyond this region has been affected but has not been captured by the mine.

Boundaries between the capture zones are moving. The recharge capture zone has been expanding downward and outward and at the current rate of dewatering it will continue to do so, thereby moving the boundary between it and the storage capture zone. The storage capture zone will also continue to expand as water mobilized many years ago reaches the mine. Eventually, the size of the storage capture zone will diminish and the recharge capture zone will expand to envelop the entire workings. Under steady conditions, the storage capture zone will be absent altogether and the deep flow system will include only recharge capture.

Cone of depression

Previous investigations (Zhan and Duex 2010; Zhan 2002; Rahn and Roggenthen 2002) have assumed that a large cone of depression was created by the mine, but this appears to be unnecessary to explain the available data. This is because the deep flow system removes only a fraction of the ambient recharge to the shallow system. A consequence of this is that even though the mine removes water like a well, it need not create the classic cone of depression around a well where the water table drops, pores are drained and an extensive vadose zone is created. This is why the water table in Fig. 7 is only slightly depressed. The authors suggest that the mine does indeed behave like a large well, but instead of being analogous to a conventional well in an aquifer with a large depressed water table, it instead resembles a well beneath a boundary created by the shallow flow system that is roughly at constant head. A reasonable analogy is a well beneath a stream or lake (Kelly and Murdoch 2003). Interestingly, despite this difference in conceptual models, the radius of influence of 2 km calculated by Zhan and Duex (2010) appears to be a reasonable estimate of the size of the region where water is captured by the mine.

Open pit

The large open pit created as part of the shallow workings was ignored when setting up the model, and simulations are able to predict the observed inflows reasonably well (Figs. 8 and 9). This suggests that the open pit has only a minor effect on the inflow used to calibrate the model, which seems reasonable in light of the small area of the pit ($\sim 0.25 \text{ km}^2$) compared to the area providing recharge to the mine workings ($\sim 25 \text{ km}^2$).

During heavy rainfall, the open pit may capture significant volumes of water that flows into the underground workings. This influx of water is expected to result in a short-lived pulse superimposed on the flows caused by groundwater. The analyses considered here are limited to inflows resulting from steady-state, distributed recharge, so effects of storm-related flows are ignored.

Permeability, stress, and the shallow flow system

The distribution of K used in the simulations (Fig. 10) was based solely on a relationship that K increases as the overburden load decreases. Our results suggest a reduction in stress on cracks or pores can explain how the rock becomes sufficiently permeable to create a shallow flow system. Many other processes may further alter K once the permeability has been increased enough to sustain substantial water flow, but the results of this work show that those other processes may be unnecessary—stress reduction alone is sufficient to create conditions required for a shallow flow system. The importance of stress-dependent permeability on the development of shallow flow systems was also recognized by Jiang et al. (2010).

Origin of mine water

The results of the simulations suggest that water seeping into the mine workings should span a broad range of ages and source areas. Water from locations near the periphery of the workings has the best chance of representing fluids native to the formation and unaffected by interactions with the workings themselves. The south side of the mine to depths of 1,600 m has the potential to be dominated by water that originated as recharge within the last 10 years, and considerably younger water (<1 year since recharge) could be infiltrating in the vicinity of the shallow workings, as well as up to 0.5 km south of the workings. Localized fractures with apertures larger than the average could be responsible for both larger than average flow rates and faster than average travel times.

Water that flows from the shallow to the deep flow system is expected to be derived primarily from the uplands between streams (Fig. 7a). The upland areas include the town of Lead and the tailings pond (Fig. 15). The composition of the water entering the southeast side of the mine could be affected by compounds from these source areas.

It is possible that water from Whitewood Creek, or another local stream, enters the mine workings. This could be significant because it could provide a mechanism for microbes or dissolved compounds to flow from surface water to the mine workings—other pathways involve the inflow of groundwater. However, the streams are at low hydraulic potential relative to the neighboring uplands, so highly transmissive features such as fractures or boreholes in precisely the right location would be required to realize this hypothetical pathway (Fig. 7). Fractures and boreholes are common in the vicinity of the former Homestake

mine, so water flow from streams to the workings cannot be dismissed.

The northwestern and lower reaches of the mine are expected to be dominated by water that was removed from storage. Flow velocities in the ambient flow system (prior to mining) at depths below 1 km are expected to have been slow, so the water stored at those depths is likely to be orders of magnitude older than the water in the recharge capture zone. The simulations suggest that water arriving at the mine today may have been several km from the mine at the time mining started, and it seems likely that the composition of the water would reflect the long residence times at depth.

Implications for deep EcoHydrology

The flow systems and hydrogeologic zones identified by this investigation (Fig. 15) are hypothesized to be a basic framework controlling the distribution and function of microbial ecosystems in the vicinity of Homestake. Fracture apertures will constrain the size of microorganisms that can be transported to depth. For the values utilized in the model above, multi-cellular eukaryotic organisms and larger protists will be restricted to the shallower zone above 100 m depth, whereas prokaryotes and smaller eukaryotes such as yeast cells like those reported from 400-m deep fractures at Äspo (Ekendahl et al. 2003) and 200-m deep aquifers at Savannah River (Sinclair and Ghiorse 1989), could penetrate to the deepest levels of the simulated region. Flow velocities and the in situ rates of aerobic microbial respiration will affect the depth to which oxygenated water can penetrate, and this will influence the distribution of microbial communities and geochemical facies.

Those fractures that are part of the recharge capture zone would likely be aerobic or hypoxic depending upon the location of their recharge zone and their microbial community would be dominated by psychrotolerant to mesophilic aerobes and facultative anaerobes along with some protists. If in situ aerobic rates are similar to those reported for the Middendorf aquifer of South Carolina, then water with subsurface residence times up to 7,000 years may still contain traces of O₂ (Phelps et al. 1994). Those fractures that are tapping into the storage capture zone, however, may contain groundwater with residence times of many thousands or more years, and be characterized by microbial communities dominated by anaerobes with few, if any, protists. At depths shallower than the 4,850L level (1480m depth), the microbial community would predominantly be mesophilic *Proteobacteria*, *Crenarchaeota* and *Euryarchaeota* (including methanogens), if the results reported from the Äspo Hard Rock Laboratory (Kotelnikova and Pedersen 1997; Pedersen 1997) and the South African Au mines (Gihring et al. 2006) where water ages are on the order of millions of years, are any guide. This hypothesis is consistent with the predominance of *Proteobacteria* in the 16S rRNA gene sequences from clone libraries of soil samples collected at

1.34 by Rastogi et al. (2009). Assuming a geothermal gradient of 20°C km⁻¹, the boreholes from the 2-km depth or deeper tapping into the storage capture zone would likely yield thermophilic anaerobes, perhaps low diversity communities dominated by members of the *Firmicutes*, since these have been found to dominate the deep subsurface biosphere in South Africa at depths greater than 2.5 km (Moser et al. 2005) and have been isolated from deep fractured rocks at other sites in the continental USA at depths greater than 2 km (Colwell et al. 1997; Liu et al. 1997a; b).

Conclusions

More than a century of dewatering has altered the hydrogeology in the vicinity of the Homestake mine in the northern Black Hills of South Dakota. Two- and three-dimensional simulations indicate that the shallow ambient flow system typical of the region is underlain by a deep flow system created by mining activities. The deep flow system includes a zone where the mine captures water originating relatively recently as recharge, and another zone where water is much older and has been released from storage in the enveloping rock. The storage capture zone has the shape of a surface-truncated ellipsoid, 8 km in maximum dimension, 4 km wide and 5 km deep.

The calibrated simulations were able to explain important hydrologic observations available from the area, including the co-existence of shallow and deep flow systems, the total flow rate pumped from the workings, and the distribution of flow and magnitude of porosity within the former mine. The simulations assumed the region was underlain by a uniform, anisotropic material whose hydrologic properties depend only on the effective stress. Equating macroscopic properties with characteristics of deformable fractures allows the number of parameters to be reduced, and it provides a physically based justification for changes in properties with depth. Reduction in stress increases hydraulic conductivity by roughly 3 orders of magnitude as the ground surface is approached, which appears to be an important feature in promoting the development of a transmissive and complex shallow flow system.

Acknowledgements We appreciate the support from the National Science Foundation under grants EAR- 0809820, EAR 0900163, CMMI 0919497, EAR 1036985, EAR 0969053 and EAR 0919357.

References

- Anderson MP, Woessner WW (1992) Applied groundwater modeling. Academic, San Diego, CA, 381 pp
- Baghbanan A, Jing L (2008) Stress effects on permeability in a fracture rock mass with correlated fracture length and aperture. Int J Rock Mech Min Sci 45:1320–1334

- Bai M, Elsworth D (2000) Coupled processes in subsurface deformation, flow and transport. American Society Civil Engineers Press, Reston, VA, 334 pp
- Bandis SC, Barton NR (1983) Fundamentals of rock joint deformation. *Int J Rock Mech Min Sci Geomech Abstr* 20:249–268
- Barenblatt GI, Zhel'tov IP, Kochina IN (1960) Basic concepts in the theory of seepage of homogeneous liquids in fissured rocks. *J Appl Math* 24:1286–1303
- Bear J (1979) *Hydraulics of groundwater*. McGraw-Hill, New York, 569 pp
- Biot MA (1941) General theory of three dimensional consolidation. *J Appl Phys* 12:155–164
- Caddey SW, Bachman RL, Otto RP (1990) "15 Ledge ore discovery, Homestake Mine, Lead, South Dakota," Proceedings of the Fourth Western Regional Conference on Precious Metals and the Environment. Lead, SD, 19–22 Sept 1990, pp 405–423
- Caddey SW, Bachman RL, Campbell TJ, Reid RR, Otto RP (1991) The Homestake Gold Mine: an early Proterozoic iron-formation-hosted gold deposit, Lawrence County, South Dakota. *US Geol Surv Bull* 1857-J, 67 pp
- Carter JM, Driscoll DG, Williamson JE, Lindquist VA (2002) Atlas of water resources in the Black Hills Area, South Dakota. *US Geol Surv Hydrol Invest Atlas HA-747*, 120 pp. <http://pubs.usgs.gov/ha/ha747/>. Cited August 2011
- Colwell FS, Onstott TC, Delwiche ME, Chandler D, Fredrickson JK, Yao Q-J, McKinley JP, Boone DR, Griffiths R, Phelps TJ, Ringelberg D, White DC, LaFreniere L, Balkwill D, Lehman RM, Konisky J, Long PE (1997) Microorganisms from deep, high temperature sandstones: constraints on microbial colonization. *FEMS Microbiol Rev* 20:425–435
- Davis AD, Webb CJ, Beaver FW (2003) Hydrology of the proposed national undergrounds science laboratory at the Homestake Mine in Lead, South Dakota, 2003 SME Annual Meeting, Cincinnati, OH, 24–26 Feb 2003, 4 pp
- Davis A, Roggenthen W, Stetler L, Hladysz Z, Johnson C (2009) Post closure flooding of the Homestake Mine at Lead, South Dakota. *Mining Eng* 61(3):43–47
- Detournay E, Cheng AH-D (1993) Fundamentals of poroelasticity. In: Hudson JA (ed) *Comprehensive rock engineering: principles, practice, projects*. V. 2. Pergamon, Oxford, UK, pp 113–171
- DeWitt ED, Redden JA, Wilson AB, Buscher D (1998) Mineral resource potential and geology of the Black Hills National Forest, South Dakota and Wyoming. *US Geol Surv* 1580, 135 pp
- Doe TW, Long JSC, Endo HK, Wilson CR (1982) Approaches to evaluate the permeability and porosity of fractured rock masses. Proceedings of the 23rd U.S. Rock Mechanics Symposium, Berkeley, CA, August 1982, pp 31–37
- Domenico PA, Mifflin MD (1965) Water from low-permeability sediments and land subsidence. *Water Resour Res* 1(4):563–576
- Driscoll DG, Carter JM (2001) Hydrologic conditions and budgets for the Black Hills of South Dakota, through water year 1998. *US Geol Surv Water Resour Invest Rep*, 143 pp
- Ekendahl S, O'Neill A, Thomsson E, Pedersen K (2003) Characterisation of yeasts isolated from deep igneous rock aquifers of the Fennoscandian shield. *Microb Ecol* 46:416–428
- Elsworth D, Bai M (1992) Flow-deformation response of dual porosity media. *J Geotech Eng Div ASCE* 118(1):107–124
- Fielder M (1970) *The treasure of Homestake gold*. North Plains, Aberdeen, SD, 478 pp
- Germanovich LN, Dyskin AV (1994) Virial expansions in problems of effective characteristics. Part I. General concepts. *Mechanics of composite materials* 30(2):157–167
- Gihring TM, Moser DP, Lin L-H, Davidson M, Onstott TC, Morgan L, Milleson M, Kieft TL, Trimarco E, Balkwill DL, Dollhopf ME (2006) The distribution of microbial taxa in the subsurface water of the Kalahari Shield, South Africa. *Geomicrobiol J* 23:415
- Gustard A, Bullock A, Dixon JM (1992) Low flow estimation in the United Kingdom. Report 108, Institute of Hydrology, Wallingford, UK
- Institute of Hydrology (1980) *Low flow studies report*. Institute of Hydrology, Wallingford, UK
- Jacob CE (1940) On the flow of water in an elastic artesian aquifer. *Trans Am Geophys Union* 22:783–787
- Jaeger JC, Cook NGW, Zimmerman R (2007) *Fundamentals of rock mechanics*, 4th edn. Wiley, New York, 469 pp
- Jiang X-W, Wan L, Cardenas MB, Ge S, Wang X-S (2010) Simultaneous rejuvenation and aging of groundwater in basins due to depth-decaying hydraulic conductivity and porosity. *Geophys Res Lett* 37:L05403. doi:10.1029/2010GL042387
- Kelly SE, Murdoch LC (2003) Well tests for determining the hydraulic conductivity of a stream bed. *Ground Water* 41(4):431–439
- Kotelnikova S, Pedersen K (1997) Evidence for methanogenic *Archaea* and homoacetogenic *Bacteria* in deep granitic rock aquifers. *FEMS Microbiol Rev* 20:339–349
- Liu SV, Zhou J, Zhang C, Cole DR, Gajdarziska-Josifovska M, Phelps TJ (1997a) Thermophilic Fe(III)-reducing bacteria from the deep subsurface: the evolutionary implications. *Science* 277:1106–1109
- Liu Y, Karnachow TM, Jarrell KE, Balkwill DL, Drake GR, Ringelberg D, Clarno R, Boone DR (1997b) Description of two new thermophilic species of *Desulfotomaculum*: *Desulfotomaculum putei* sp. nov. from the deep terrestrial subsurface and *Desulfotomaculum luciae* sp. nov. from a hot spring. *Int J Syst Bacteriol* 47:615–621
- Mitchell ST (2009) *Nuggets to neutrinos: the Homestake Story*. Xlibris, Bloomington, IN, 738 pp
- Moser DP, Gihring TM, Brockman FJ, Fredrickson JK, Balkwill DL, Dollhopf ME, Sherwood-Lollar B, Pratt LM, Boice EA, Southam G, Wanger G, Baker BJ, Pfiffner SM, Lin L-H, Onstott TC (2005) *Desulfotomaculum* spp. and *Methanobacterium* spp. dominate 4–5km deep fault. *Appl Environ Microbiol* 71:8773–8783
- Murdoch LC, Germanovich L (2006) Analysis of a deformable fracture in a permeable material. *Int J Numer Anal Methods Geomech* 30:529–561
- Pariseau W (1985) Research study on pillar design for vertical crater retreat (VCR). Bureau of Mines Contract Report J0215043, US Bureau of Mines, Washington, DC
- Pedersen K (1997) Microbial life in deep granitic rock. *FEMS Microbiol Rev* 20:399–414
- Phelps TJ, Murphy EM, Pfiffner SM, White DC (1994) Comparison between geochemical and biological estimates of subsurface microbial activities. *Microb Ecol* 28:335–349
- Rahn PH (1985) Ground water stored in the rocks of western South Dakota. In: Rich FJ (ed) *Geology of the Black Hills, South Dakota and Wyoming*, 2nd edn. Geological Society of America, Field Trip Guidebook, American Geological Institute, Alexandria, VA, pp 154–174
- Rahn PH, Johnson CS (2002) Effects of anisotropic transmissivity on a contaminant plume at Nemo, South Dakota: environ. *Eng Geosci* VIII(1):11–18
- Rahn P, Roggenthen W (2002) Hydrogeology of the Homestake Mine. *Proc South Dakota Acad Sci* 81:19–25
- Rastogi G, Stetler LD, Peyton BM, Sani RK (2009) Molecular analysis of prokaryotic diversity in the deep subsurface of the former Homestake gold mine, South Dakota, USA. *J Microbiol* 47:371–384
- Rutqvist J (1995) Determination of hydraulic normal stiffness of fractures in hard rock from hydraulic well testing. *Int J Rock Mech Min Sci Geomech Abstr* 32:513–523
- Rutqvist J, Stephansson O (2003) The role of hydromechanical coupling in fractured rock engineering. *Hydrogeol J* 11:7–40
- Rutqvist J, Tsang C-F, Stephansson O (1997) Hydraulic field measurements of incompletely closed fractures in granite. *Int J Rock Mech Min Sci Geomech* 34:411
- Rutledge AT (1998) Computer programs for describing the recession of ground-water discharge and for estimating mean ground-water recharge and discharge from stream-flow data. *US Geol Surv Water Resour Invest Rep* 98–4148, 43 pp

- Sinclair JL, Ghiorse WC (1989) Distribution of aerobic bacteria, protozoa, algae and fungi in deep subsurface sediments. *Geomicrobiol J* 7:15–31
- Svenson ET, Schweisinger L, Murdoch (2007) Analysis of the hydromechanical response of a flat-lying fracture to a slug test. *J Hydrol* 347:35–47
- Toth J (1963) A theoretical analysis of ground water flow in small drainage basins. *J Geophys Res* 68(16):4795–4812
- Wang HF (2000) *Theory of linear poroelasticity*. Princeton University Press, Princeton, NJ, 281 pp
- Wang HF, Anderson MP (1982) *Introduction to groundwater modeling: finite difference and finite element methods*. Freeman, Reston, VA, 237pp
- Warren JE, Root PJ (1963) Behavior of naturally fractured reservoirs. *SPE J* 3(3):245–255
- Zhan J (2002) Homestake Mine open cut evaluation of the pit water recovery. Internal report, Homestake Mining Company, Lead, SD, 17 pp
- Zhan G, Duex T (2010) Hydrologic evaluation of post-closure flooding and dewatering of the Homestake Mine. *Mining Eng* 62(4):64–68